JOURNAL OF MATERIALS SCIENCE 17 (1982) 3149–3157

Thermal fatigue life of ceramics under mechanical load

N. KAMIYA, O. KAMIGAITO
Toyota Central Research and Development Laboratories, 41-1 Aza Yokomichi, Oaza Nagakute, Nagakute-cho, Aichi-gun, Aichi-ken, 480-11 Japan

Thermal fatigue life of ceramics under mechanical load was studied using a soda-lime–silica glass rod. The life was also calculated by the application of fracture mechanics of ceramics based on slow crack growth. Both results agreed well. For instance, the following formulae hold well for the fatigue life of the ceramics under mechanical stress:

$$\ln(-\ln P) \doteqdot \frac{m}{n}\ln N + \frac{lm}{n}\ln\sigma_{MO} + \frac{(n-l)m}{n}\ln(\Delta T) + C'$$

$$\frac{l}{(n-l)} \doteqdot \frac{\sigma_{MO}}{\sigma_{TO}}$$

where P, N, σ_{TO}, σ_{MO}, ΔT, m, n and l and C' are survival probability, thermal stressing cycles (thermal fatigue life), the maximum thermal stress, mechanical stress, thermal shock severity, Weibull modulus, a material constant and constants, respectively. By the application of the second formula, the thermal stress induced on the glass rod in plunging the rod into water from hot atmosphere was estimated. The estimated value (11.2 kg mm^{-2} for a glass rod of 4 mm diameter and $\Delta T = 180°$ C) is thought to agree rather well with that estimated from the well-known formula derived from heat diffusion theory (9.7 ~ 15.8 kg mm^{-2}) considering the accuracy of the approximation.

1. Introduction

It has been shown that the prediction of fatigue life of ceramics can be made by application of fracture mechanics of ceramics in the absence of mechanical load [1, 2]. In practice, however, thermal fatigue frequently occurs under the influence of mechanical load. Thus, the prediction of thermal fatigue life of ceramics in the presence of mechanical load is as important as that of ceramics in the absence of the load. In the present paper, this has been studied using a soda–lime–silica glass rod.

2. Experimental procedure

2.1. Specimens

Soda-lime–silica glass rods were chosen for the experiment. Their dimensions were 4 mm in diameter and 75 mm in length. The specimens were cut from a long bar with a diamond blade. The ends of each rod were protected with tubes of glass fibre to prevent them initiating failure.

2.2. Apparatus

The glass rods were subjected to thermal shock using the apparatus shown in Fig. 1. Nine rods were loaded in the specimen holder, and three-point bending stress was applied to each rod through a fine stainless wire connected to a weight (Fig. 1). The rods were kept for 30 min in a furnace, then plunged rapidly into water at 30 ± 0.5° C. The time for the transfer from the furnace to water was about 1.6 sec. A spring was used to relax the stress induced by the rapid motion of the specimen and weights in plunging. The increment in the stress due to the motion for the immersion was within 10% of that due to the weight, which was measured with a strain gauge set on a glass rod. After the immersion of 5 min, the specimens were slowly transfered into the furnace. The time for the transfer was about

0022–2461/82/113149–09$03.58/0

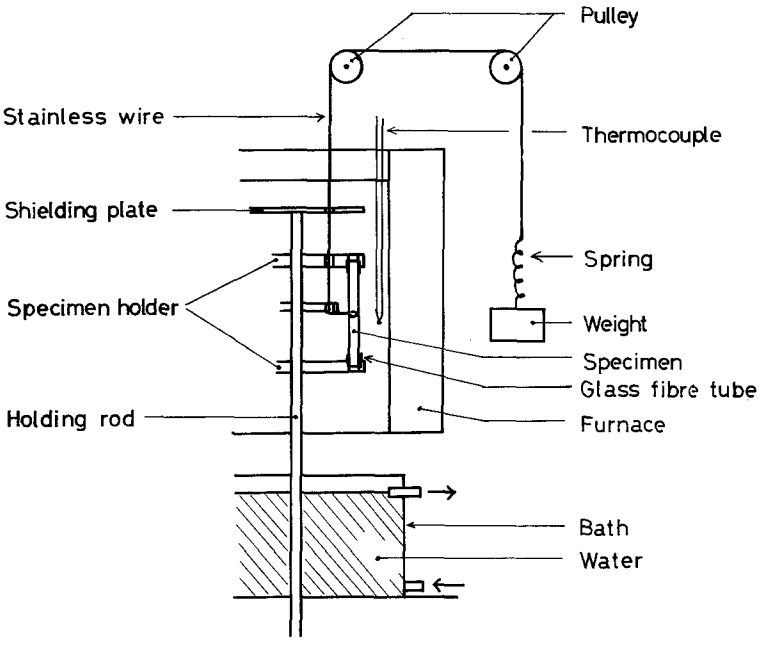

Figure 1 Schematic diagram of the thermal fatigue testing apparatus. Mechanical stress is induced through a wire by a weight.

16 sec. The heating and cooling process was repeated until all specimens were broken. The number of cycles at which each specimen broke was recorded on a digital counter connected to each stainless wire.

The thermal shock severity, ΔT, i.e. the temperature difference between the furnace and the water, was varied from 210° C to 180° C. In water quenching, however, as water vapour is apt to envelop the specimen in water, it is desirable to take ΔT as that between the temperature of the hot zone and the boiling point of water, 100° C, as pointed out by Davidge and Tappin [3]. From these considerations ΔT was taken in the present paper as that between the temperature of the hot zone and that of water, ΔT_{30} (base temperature = water temperature), as well as that between the temperature of the hot zone and 100° C, ΔT_{100} (base temperature = 100° C), and the results in both systems of ΔT have been examined. The mechanical stress level, σ_{MO}, was varied from 2.28 to 0.554 kg mm^{-2}.

The flexural strength of the glass rod was measured by applying three-point loading to the span of 40 mm length at room temperature and the Weibull modulus was compared with that determined from the failure by thermal fatigue in the presence of mechanical stress. To examine the value of exponent, n, in the formula $V = A k_I^n$, the stress rate was varied from 6.66 to 6.66 x 10^{-2} kg mm^{-2} sec^{-1}, where V, A and K_I stand respectively for the crack velocity, a material constant and the stress intensity factor. The value of n was given through the following formula:

$$\left(\frac{\sigma_f}{\sigma_f'}\right) = \left(\frac{\dot{\sigma}}{\dot{\sigma}'}\right)^{\frac{1}{n+1}}$$

where σ_f and σ_f' stand respectively for the medians of the flexural strength under the stressing rates of $\dot{\sigma}$ and $\dot{\sigma}'$. The value of n was compared with that determined from the thermal fatigue experiment.

3. Results

3.1. Thermal fatigue

The survival probability, P, at a given mechanical stress level (0.554 kg mm^{-2}) is plotted as a function of the cycles of thermal stressing (thermal fatigue life), N, in Fig. 2. P was calculated by the equation $P = 1 - F = 1 - (i - 0.3)/(J + 0.4)$, where F is the cumulative failure probability for specimen i from an ordered set of J specimens. In this test, the number of specimens was 18 for each experimental condition. P at various mechanical stress levels is given in Fig. 3 for a fixed value of ΔT. As shown in Figs 2 and 3, $\ln(-\ln P)$ plotted against $\ln N$ for fixed values of ΔT and σ_{MO} gives a straight line obtained by a linear regression analysis according to a linear relation between $\ln(-\ln P)$ and $\ln N$, and the lines for different values of ΔT and σ_{MO} are almost parallel to one another. These features resemble those in T–SPT (thermal

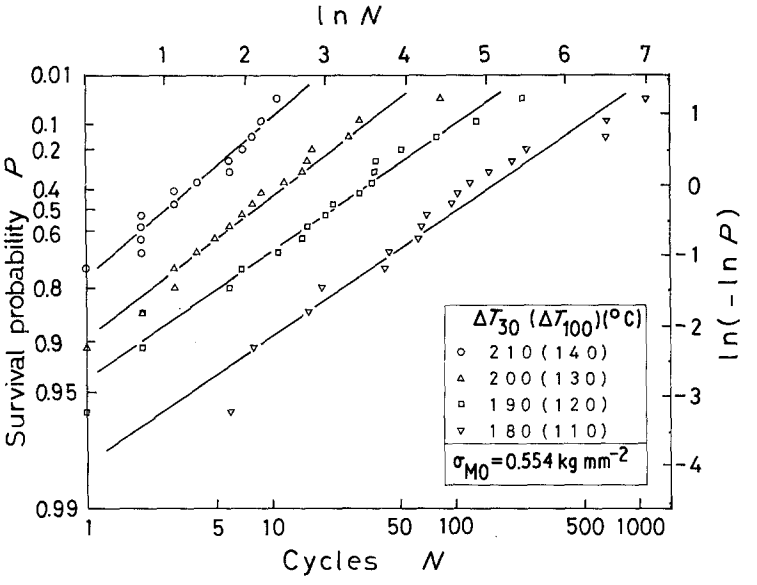

Figure 2 The survival probability, P, as a function of the number of thermal stressing cycles, N, under a constant value of mechanical stress (0.554 kg mm^{-2}) for soda-lime–silica glass. Linear lines are obtained by a linear regression analysis.

shock severity–probability–time) diagrams [2], and the possibility of a similar formulation to T–SPT diagrams based on fracture mechanics of ceramics is suggested for the present study. This will be discussed later.

3.2. Flexural strength

The survival probability, P $(= 1 - (i - 0.3)/(J + 0.4), J = 40)$, is plotted as a function of flexural strength, σ_f, for various stressing rates in Fig. 4. As shown in the figure, it fits a straight line which was obtained by a linear regression analysis according to a linear relation between $\ln(-\ln P)$ and $\ln \sigma_f$. The Weibull moduli, m, determined from the linear regression analysis are 9.0 ± 0.2, 9.6 ± 0.4, 9.0 ± 0.5 and 8.3 ± 0.2 under a stressing rate of 6.66×10^{-2}, 6.66×10^{-1}, 2.66 and 6.66 kg mm^{-2} sec^{-1}, respectively. Flexural strengths at $P = 0.5$ are given by 13.3, 15.8, 17.1 and 16.8 kg mm^{-2}, respectively. The values of m determined above are in good agreement with those given by other authors for soda–lime–silica glass [4]. From the dependence of the flexural strength at which P is 0.5 on the stressing rate, the material constant, n, is estimated as $n = 17.2 \pm 4.0$, which is in good agreement with the literature value [5].

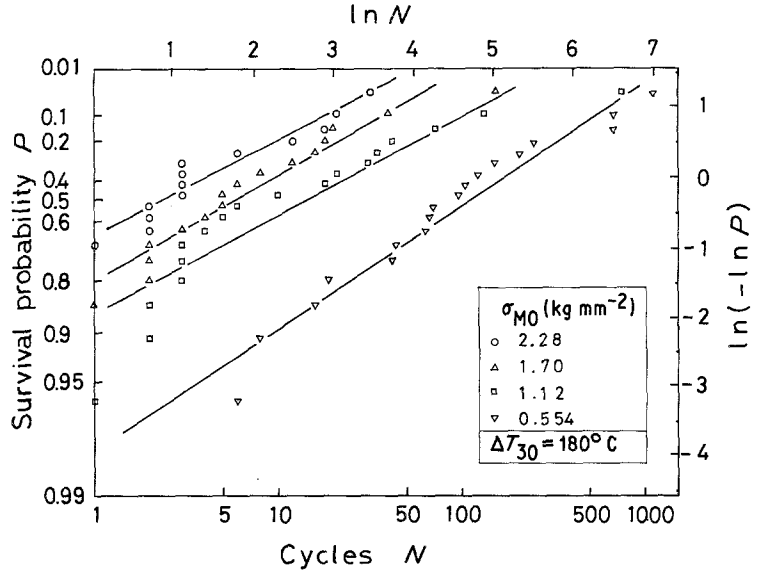

Figure 3 The survival probability, P, as a function of the thermal stressing cycles, N, at a fixed value of ΔT_{30} (180° C) for soda-lime–silica glass. Linear lines are obtained by a linear regression analysis.

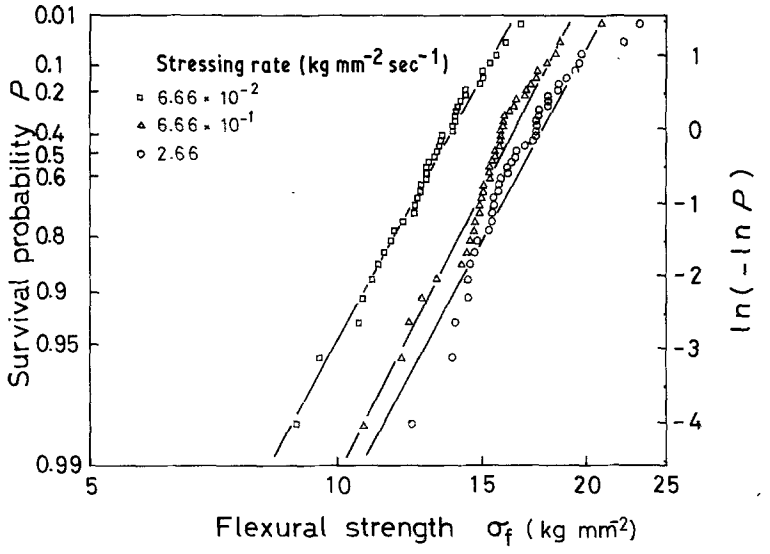

Figure 4 Flexural strength distribution of soda-lime–silica glass for various stressing rates. Linear lines are obtained by a linear regression analysis.

4. Discussion

As suggested before, the thermal fatigue in the presence of mechanical stress is expected to be treatable using the same approximation as that used in the absence of stress. On the basis of fracture mechanics, the crack-growth rate, V, is expressed as follows [6]:

$$V = \frac{da}{dt} = A K_I^n \tag{1}$$

where a and t stand respectively for the crack length and time, and the other variables are explained above. Furthermore, K_I is expressed as follows [7]:

$$K_I = Y \sigma a^{1/2} \tag{2}$$

where Y and σ stand respectively for a geometrical factor and stress. From Equations 1 and 2, V is expressed as follows:

$$V = \frac{da}{dt} = A Y^n \sigma^n a^{n/2}. \tag{3}$$

For a ceramic under thermal stress in the presence of a mechanical stress, σ is composed of the thermal stress, σ_T, and the mechanical stress, σ_M. Therefore, the following equation holds:

$$\frac{da}{dt} = A Y^n (\sigma_T + \sigma_M)^n a^{n/2}. \tag{4}$$

In general, Y, σ_T and σ_M depend on a as well as t and temperature, and it is almost impossible to get an exact solution of Equation 4. For a rough evaluation of the failure time, however, they can be approximated to be independent of a, as the fatigue life is almost dominated by the duration in which a reaches a certain small and critical length. Moreover, their dependence on temperature can be approximated by assuming that the temperature is almost constant [2]. From this approximation, the following equation can be derived:

$$a_i^{(2-n)/2} - a^{(2-n)/2} = \left(\frac{n-2}{2}\right) A Y^n \times \left\{ \sum_{q=0}^{n} nCq \int_0^t \sigma_M^q \, \sigma_T^{n-q} \, dt \right\} \tag{5}$$

where a_i stands for the initial crack length. In most cases, σ_M as well as σ_T varies periodically with time. On this consideration, a at the end of N cycles can be expressed as follows:

$$a_i^{(2-n)/2} - a^{(2-n)/2} = \left(\frac{n-2}{2}\right) A Y^n N \times \left\{ \sum_{q=0}^{n} nCq \int_0^{\omega} \sigma_M^q \, \sigma_T^{n-q} \, dt \right\} \tag{6}$$

where ω is the periodic time of the thermal cycle. At the occurrence of failure, $a \gg a_i$. Therefore the following equation is derived from Equation 6:

$$a_i^{(2-n)/2} \doteqdot \left(\frac{n-2}{2}\right) A Y^n N \times \left\{ \sum_{q=0}^{n} nCq \int_0^{\omega} \sigma_M^q \, \sigma_T^{n-q} \, dt \right\}. \tag{7}$$

Moreover, σ_T is proportional to the thermal shock severity, ΔT, on the assumption that the temperature difference is limited to a narrow range [2]. Therefore σ_T is expressed as follows:

$$\sigma_T = \sigma_{TO} f(t) = k \Delta T f(t) \quad (8)$$

where σ_{TO} and k stand for the maximum stress and a constant, respectively, and $f(t)$ is a function of time whose maximum is normalized to unity. σ_M can also be expressed as follows:

$$\sigma_M = \sigma_{MO} g(t) \quad (9)$$

where σ_{MO} stands for the maximum sress and $g(t)$ is a function of time whose maximum is normalized to unity. Substitution of Equations 8 and 9 into Equation 7 gives the following:

$$a_i^{(2-n)/2} \doteqdot \left(\frac{n-2}{2}\right) A Y^n N \times \left\{\sum_{q=0}^{n} nCq\, \sigma_{MO}^q\, (k\Delta T)^{n-q} \int_0^{\omega} g^q f^{n-q}\, dt\right\}. \quad (10)$$

The right-hand side of Equation 10 consist of many terms involving different exponents of σ_{MO} as well as ΔT. It, however, can be well approximated by the assumption that the main contribution of σ_{MO} comes from the maximum term and others in Equation 10 (see the Appendix). The maximum term is given by the values of q, l, which are determined by the following equation (Appendix):

$$\frac{l}{n-l} \doteqdot \frac{\sigma_{MO}}{\sigma_{TO}} = \frac{\sigma_{MO}}{k\Delta T}. \quad (11)$$

Therefore, the following is given:

$$a_i^{(2-n)/2} \doteqdot \gamma\left(\frac{n-2}{2}\right) \times A Y^n N_n C_l \sigma_{MO}^l \sigma_{TO}^{n-l} H\left(l, \frac{\sigma_{MO}}{\sigma_{TO}}\right) \quad (12)$$

where γ is a constant, and

$$H\left(l, \frac{\sigma_{MO}}{\sigma_{TO}}\right) = \int_0^{\omega} g^l f^{n-l}\, dt. \quad (13)$$

On the basis of Weibull statistics, the distribution of the initial crack length in ceramics can be expressed as follows [2]:

$$P = \exp\left[-V(a_i/a_0)^{-m/2}\right] \quad (14)$$

where V, a_0 and m stand respectively for the stressed volume, normalization constant and Weibull modulus. Substitution of Equation 12 into Equation 14 gives the following:

$$\ln(-\ln P) \doteqdot \frac{m}{n}\ln N + \frac{lm}{n}\ln\sigma_{MO} + \frac{(n-l)m}{n}\ln\sigma_{TO} + C \quad (15)$$

or

$$\ln(-\ln P) \doteqdot \frac{m}{n}\ln N + \frac{lm}{n}\ln\sigma_{MO} + \frac{(n-l)m}{n}\ln(\Delta T) + C' \quad (16)$$

where

$$C = V a_0^{m/2}\left\{\left(\frac{n-2}{2}\right)\gamma A Y_n C_l H\right\}^{m/(n-2)}$$

$$C' = C k^{(n-l)m/(n-2)}.$$

Equations 15 and 16 prove a nearly linear dependence of $\ln(-\ln P)$ on $\ln N$ and also on $\ln(\Delta T)$ or $\ln\sigma_{MO}$. The equations prove the occurrence of the parallel shift of the line made by $\ln(-\ln P)$ plotted against $\ln N$, with the variation of ΔT as well as σ_{MO}. These results agree well with the experimental results mentioned before.

According to the equations, $\ln(-\ln P)$ plotted against $\ln N$ gives the value of m/n as its tangent. For a given value of P, $\ln N$ plotted against $\ln\sigma_{MO}$ gives the value of l, and that plotted against $\ln(\Delta T)$ gives the value of $(n-l)$.

In Figs 5 and 6, the value of $\ln N$ for $P = 0.5$ on each line in Figs 2 and 3 is plotted respectively against $\ln(\Delta T)$ and $\ln\sigma_{MO}$. The set of experimental data are fitted to a straight line obtained by a linear regression analysis according to Equation 16 in either case. This proves Equation 15 and 16 valid. The value of l determined from the tangent of the straight line in Fig. 6 is 2.6 ± 0.1. The values of $(n-l)$ determined from Fig. 5 are 23.3 ± 1.3 for ΔT_{30} and 14.9 ± 0.8 for ΔT_{100}. These values give 25.9 ± 1.3 and 17.5 ± 0.8 as the value of n for ΔT_{30} and ΔT_{100}, respectively. The value of n determined by taking the base temperature as that of boiling water agrees with the literature value [5] than the other system of ΔT, in which the base temperature is that of water, 30° C. However, since the difference of the value of n in the two systems is small, the determination of a more suitable system of the two systems was impossible in the present experiment. A more suitable system

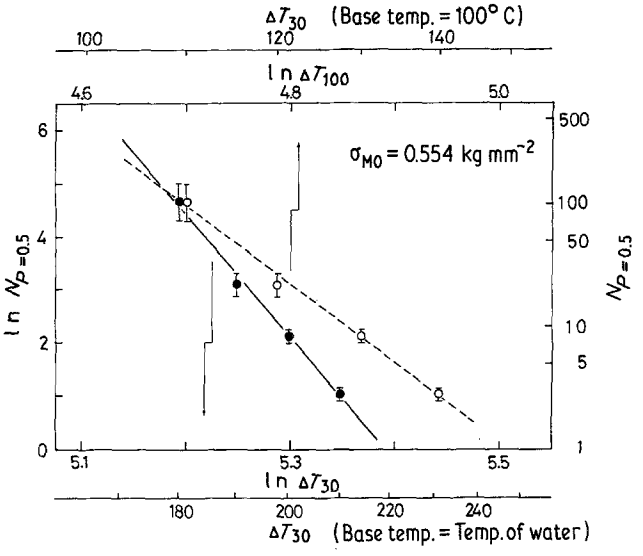

Figure 5 Dependence of the median of thermal fatigue life, N, on thermal shock severity, ΔT, for soda-lime–silica glass under constant mechanical stress (σ_{MO} = 0.554 kg mm^{-2}). Circles correspond to the value of N for $P = 0.5$ on each line shown in Fig. 2.

other than the two systems of ΔT may be determined from further experiments in which oil could be used as a cooling medium. From these results and the slope of each line in Figs 2 and 3, m is determined according to Equation 16, and is shown in Table I, together with the value determined from the mechanical method (flexural strength data). The value given by the thermal fatigue data is a little higher than the value given by mechanical stressing. The failure occurred normal to the rod in either case. Therefore the discrepancy between the values of m determined separately cannot be attributed to the possible difference in the distribution of flaws in the normal and parallel directions to the glass rod as in the failure in the absence of mechanical stress [2].

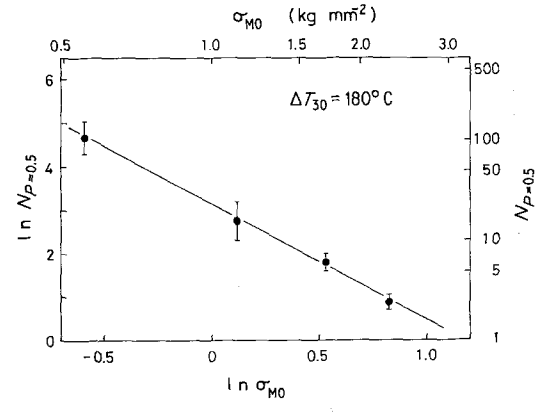

Figure 6 Dependence of the median of thermal fatigue life, N, on mechanical stress, σ_{MO}, for soda-lime–silica glass for the fixed value of ΔT_{30}, 180° C (ΔT_{100}, 110° C). Circles correspond to the value of N for $P = 0.5$ on each line shown in Fig. 3.

The occurrence of different values of m for separate failure processes is also reported by Bansal *et al.* [8] for sintered alumina in which m ranges from 11 to 34, and also for hot pressed alumina in which m ranges from 6 to 17. Therefore, it might be considered that the value of m is not always the same for separate failure processes, or that there are many types of flaws having different values of m, one of which is sensitive to some limited failure processes and environments and others which are sensitive to others. Occurrence of such flaws, however, cannot be accepted for glass or similar materials, at least because there is a close correspondence between the sequence of the thermal fatigue life in thermal quenching of glass rods and that of mechanical strength measured in ambient atmosphere of the rods [9]. Therefore, the large value of m given for the fatigue life is thought to result from the larger effective area for the thermal stress than that for mechanical stress.

A life prediction diagram of thermal fatigue is drawn in Figs 7 and 8, based on Equation 16 and the parameter determined experimentally. The values of parameters m, n, l and C' are 22.9, 25.9, 2.6 and 91.1 respectively, and the values of m and C' are those determined from the linear regression analysis of thermal fatigue data under the condition of $\Delta T_{30} = 180°$ C and σ_{MO} = 0.554 kg mm^{-2}. As shown in Figs 7 and 8, thermal fatigue data agree well with the predicted line.

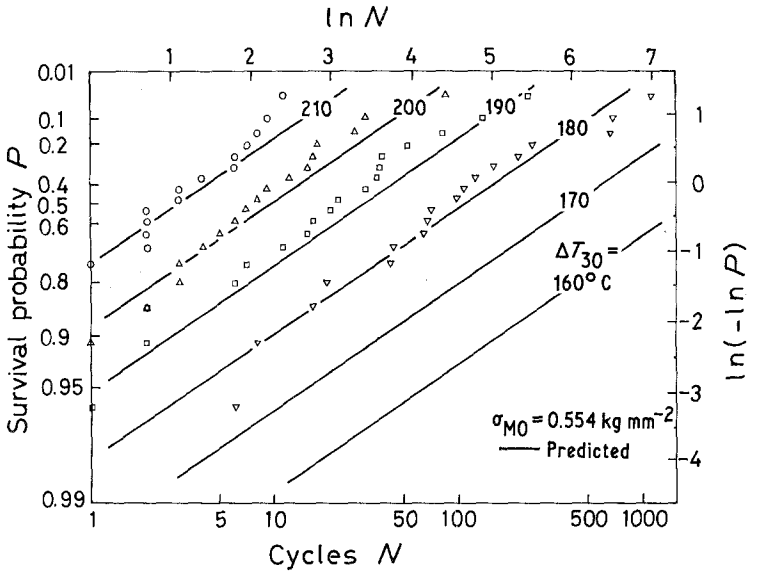

Figure 7 Life prediction diagram of thermal fatigue of soda-lime–silica glass rod under a constant mechanical stress (0.554 kg mm^{-2}). Parameter indicates the temperature difference, ΔT_{30}. For comparison, experimental data are also shown.

These show that Equation 16 is valid, and that diagrams such as Figs 7 and 8 are very useful for the prediction of thermal fatigue life of ceramics.

According to Equation 11, the maximum thermal stress, σ_{TO}, can be determined from the value of n, l and σ_{MO}. By the use of n and l determined by Figs 5 and 6 and of 1.26 kg mm^{-2} as the value of σ_{MO} determined by averaging the logarithm of the minimum and maximum applied stress in Fig. 6 (= (ln 0.554 + ln 2.28)/2), σ_{TO} was determined as 11.2 kg mm^{-2} for $\Delta T_{30} = 180°$ C ($\Delta T_{100} = 110°$ C). It is given in Table II together with the value given from the formula [10]:

$$\sigma_{TO} = \frac{E\alpha}{1-\mu}(T_a - T_s) \qquad (17)$$

where E, α, μ, T_a and T_s stand respectively for Young's modulus, the linear coefficient of thermal expansion, Poisson's ratio, and the average and surface temperatures ($E = 6.9 \times 10^{10}$ N m^{-2}, $\alpha = 9.5 \times 10^{-6}$ C^{-1}, $\mu = 0.24$).

As listed in Table II, the value given through Equation 11 is intermediate between the values given through Equation 17 as $\Delta T_{30} = 180°$ C (base temperature = temperature of water) and $\Delta T_{100} = 110°$ C (base temperature = boiling tem-

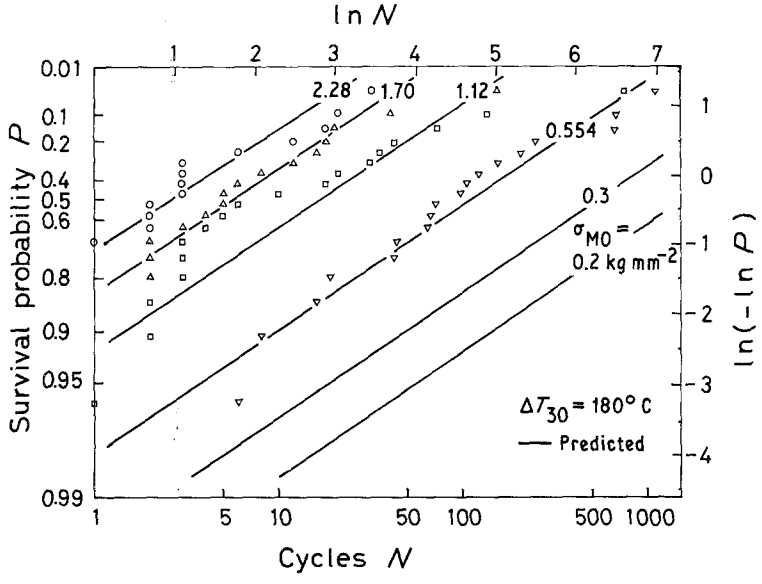

Figure 8 Life prediction diagram of thermal fatigue of soda-lime–silica glass rod under a constant temperature difference, $\Delta T_{30} = 180°$ C. Parameter indicates the constant mechanical stress. For comparison, experimental data are also shown.

TABLE I Value of m determined from the thermal fatigue data (Figs 2 and 3) and the flexural strength data (Fig. 4)

ΔT_{30} (ΔT_{100}) (° C)	σ_{MO} (kg mm^{-2})	m	
		From thermal* fatigue data	From flexural strength data
180 (110)	2.28	17.2 (3.1)†	
180 (110)	1.70	18.9 (3.2)	
180 (110)	1.12	18.1 (3.4)	
180 (110)	0.554	22.9 (3.8)	9.0 (0.2)†
190 (120)	0.554	23.1 (3.7)	
200 (130)	0.554	25.7 (4.1)	
210 (140)	0.554	28.5 (4.8)	

*Obtained by combination of the value of n, 25.9, determined from Figs 5 and 6, with m/n determined from Figs 2 and 3.
†The numbers in parentheses represent the standard deviation.

perature of water). This shows that the value given through Equation 11 is reasonable and Equation 11 is valid. Therefore, it seems to be correct to calculate the temperature difference, ΔT, by a formula as follows:

$$\Delta T = \Delta T_{100} + \eta(100 - T_w) \quad (18)$$

where $0 < \eta < 1$ and T_w is the temperature of the water cooling medium. A more precise value of η should be determined by further experiments.

The estimated value of σ_{TO} (11.2 kg mm^{-2}) is much higher than the value of σ_{MO} (1.26 kg mm^{-2}), which proves the consistency of the application of the equations to the analysis. From these good agreements, the validity of the formula derived on the basis of the fracture mechanics of ceramics is proved. These formulae will be applicable to ceramics other than glass, when either thermal stress or mechanical stress is much larger than other stresses.

Equations 15 and 16 show that the T–SPT diagram [2] holds for the ceramics thermally stressed in the presence of mechanical stress, in which the value of m must be taken as that estimated in a similar environment. In the diagram, details are somewhat different from that in the absence of mechanical stress. In the absence of the stress, the tangent of the line made by plotting $\ln(-\ln P)$ against $\ln N$ is common to any value of ΔT. But in the presence of stress, the maximum term in the right-hand side of Equation 10, or l varies slowly with variation of ΔT. It causes the variation of the tangent of the line plotted against $\ln N$ with $\ln \Delta T$. Therefore, the validity of the parallel shift of the line with the variation of ΔT is limited to only a small range of ΔT.

TABLE II Values of thermal stresses estimated by the present thermal fatigue data (Equation 11) and estimated with the heat diffusion theory

σ_{TO} (kg mm^{-2})		ΔT (° C)
Present data (Equation 11)	Heat diffusion theory* (Equation 17)	
11.2 (0.7)†	15.8	180 (ΔT_{30})
	9.7	110 (ΔT_{100})

*Gives the value $E = 6.9 \times 10^{10}$ N m^{-2}, $\alpha = 0.5 \times 10^{-6}$ ° C^{-1} and $\mu = 0.24$, which are the values for soda-lime–silica glass used.
†The numbers in parentheses represent the standard deviation.

5. Conclusions

(a) Some formulae for prediction of thermal fatigue life of ceramics in the presence of mechanical stress are given.

(b) The formulae are proved to be valid by experiments on soda-lime–silica glass.

(c) By using one of the formulae, thermal stress induced on the glass rod in water-quenching is estimated as 11.2 kg mm^{-2}, which is in good agreement with the value estimated by a formulae based on heat diffusion theory (9.7 ~ 15.8 kg mm^{-2}).

Appendix

For evaluation of the contribution of σ_{MO} to Equation 10, $L(q)$ is defined as follows:

$$L(q) = \frac{n!}{q!\,(n-q)!}\,\sigma_{MO}^{q}\,\sigma_{TO}^{n-q}\int g^{q} f^{n-q}\,dt. \quad (A1)$$

By taking q as a continuous variable, the maximum of $L(q)$ is approximately given by equating its derivative to zero:

$$\frac{d \ln L(q)}{dq} = 0 = -\ln\frac{q}{n-q} + \ln\frac{\sigma_{MO}}{\sigma_{TO}} + \frac{d}{dq}\left\{\ln\left(\int g^q f^{n-q}\, dt\right)\right\}. \quad (A2)$$

The last term on the right-hand side of Equation A2 gives the following:

$$\frac{d}{dq}\left\{\ln\left(\int g^q f^{n-q}\, dt\right)\right\} = Z = \frac{1}{\int g^q f^{n-q}\, dt} \left\{\int (\ln g) g^q f^{n-q}\, dt - \int (\ln f) g^q f^{n-q}\, dt\right\}. \quad (A3)$$

When $g = l$, or σ_M is constant:

$$Z = -\frac{\int (\ln f) f^{n-q}\, dt}{\int f^{n-q}\, dt}. \quad (A4)$$

In most cases, f is a rapidly changing function of time which has the maximum, and the maximum is normalized to unity by the definition. Therefore f^{n-q} is almost zero outside the vicinity of the time at which f is unity or the maximum. The value of $\ln f$ is zero at the time, and large in the region where f^{n-q} is almost zero. Therefore, Z is considered to be very small and can be neglected in Equation A2 for determining the maximum, because $\ln \{q/(n-q)\}$ and $\ln (\sigma_{MO}/\sigma_{TO})$ are not always small.

When g is a function of t which has the maximum, a similar result is given. Therefore, approximated values of q, l, which give the maximum term in Equation 10, are given by neglecting the integral factor as follows:

$$\frac{l}{n-l} \doteqdot \frac{\sigma_{MO}}{\sigma_{TO}} \quad (A5)$$

As shown above, the main contribution of σ_{MO} comes from the terms having the factor, $nCq\,\sigma_{MO}^{q}\,\sigma_{TO}^{n-q}$, of comparably large value. These terms with large values are evidently those having the value of q which is nearly the same with the value of l, because $nCq\,\sigma_{MO}^{q}\,\sigma_{TO}^{n-q}$ is nearly the same as the maximum value, ${}_nC_l\,\sigma_{MO}^{l}\,\sigma_{TO}^{n-l}$, when $q \doteqdot l$ and it decreases rapidly when the deviation of q from l exceeds a certain value. Moreover, the value of $nCq\,\sigma_{MO}^{q}\,\sigma_{TO}^{n-q}$ as a function of q is approximately symmetric around the value of l, or ${}_nC_{l-\Delta l}\,\sigma_{MO}^{l-\Delta l}\,\sigma_{TO}^{n-l+\Delta l} = {}_nC_{l+\Delta l}\,\sigma_{MO}^{l+\Delta l}\,\sigma_{TO}^{n-l-\Delta l}$. From these considerations, $a_i^{(2-n)/2}$ in Equation 10 can be approximated as follows:

$$a_i^{(2-n)/2} \doteqdot \left(\frac{n-2}{2}\right) A Y^n N \sum_{q=l-\Delta l}^{q=l+\Delta l} {}_nC_q\,\sigma_{MO}^{q}\,\sigma_{TO}^{n-q} \times \int_0^{\omega} g^q f^{n-q}\, dt \quad (A6)$$

$$\doteqdot \gamma \left(\frac{n-2}{2}\right) A Y^n N_n C_l \sigma_{MO}^{l}\,\sigma_{TO}^{n-l} \times \int_0^{\omega} g^l f^{n-l}\, dt \quad (A7)$$

($\gamma = 2\Delta l$: constant).

The approximation, Equation A7, is confirmed to be good referring to the derivative, $da_i^{(2-n)/2}/d\sigma_{MO}$, also, because the derivative given from Equation A6 by the use of the approximation adopted for the derivation of Equation A6 is the same as that given by directly derivating Equation A7 as to σ_{MO}.

References

1. N. KAMIYA and O. KAMIGAITO, *J. Mater. Sci.* **13** (1978) 212.
2. *Idem, ibid.* **14** (1979) 573.
3. R. W. DAVIDGE and G. TAPPIN, *Trans. Brit. Ceram. Soc.* **66** (1967) 405.
4. D. P. H. HASSELMAN, R. BADALIANCE, K. R. McKINNEY and C. H. KIM, *J. Mater. Sci.* **11** (1976) 458.
5. S. M. WIEDERHORN and L. H. BORZ, *J. Amer. Ceram. Soc.* **53** (1970) 543.
6. A. G. EVANS, "Fracture Mechanics of Ceramics 1" (Plenum Press, New York, 1976) p. 17.
7. P. C. PARIS and G. C. SIH, *ASTM SPECIAL Tech. Publ.* No. 381 (1965).
8. G. K. BANSAL and W. H. DUCKWORTH, "Fracture Mechanics of Ceramics 3" (Plenum Press, New York, 1978) p. 189.
9. N. KAMIYA and O. KAMIGAITO, *J. Mater. Sci.* **16** (1981) 828.
10. W. D. KINGERY, H. K. BOWEN and D. R. UHLMANN, "Introduction to Ceramics" 1st edn (John Wiley and Sons, New York, 1967) p. 632.

Received 1 April 1981
and accepted 22 March 1982